Available online at www.sciencedirect.com

SciVerse ScienceDirect

Procedia Computer Science 10 (2012) 136 – 143

Procedia Computer Science

The 3rd International Conference on Ambient Systems, Networks and Technologies (ANT)

Ultrasonic Non-Destructive Testing (NDT) Using Wireless Sensor Networks

Ahmad El Kouche, Hossam S. Hassanein

School of Computing, Queen's University, Kingston, ON, Canada

Abstract

This paper describes the integration of an ultrasonic-based non-destructive testing (NDT) with wireless sensor networks (WSNs) to continuously monitor material integrity during run-time. NDT is a technique that allows the examination of material properties without causing any damage to the material in the process. A wireless sensor network facilitates the collaborative effort to monitor a certain aspect without the need for expensive wired infrastructures. In this paper we describe the system architecture of a NDT system that is ultra low power, low cost, easy to use, and autonomously integrates into our WSN platform to collaboratively monitor the status conditions of industrial equipment. Our system was successfully deployed to monitor the thickness of a compound-metal (tungsten and steel) sheets used in vibration screens, which are utilized in the harsh industrial environments of the Oil-Sands, located in northern Alberta, Canada. The integration of the two technologies, WSN-based NDT, will bring about new applications in the field of low cost wireless material examination in real-time.

Non-destructive testing; NDT; WSN; Modular; System Architecture; Industrial; Harsh Environment; Equipment Monitoring; Material Thickness;

1. Introduction

Non-destructive testing is a widely used technique to validate or monitor material without compromising the integrity of the material. Ultrasound-waves are widely used in this technique due to the different behavior an ultrasound wave exhibits in various material properties. Sound waves that are beyond the maximum hearing threshold of humans are categorized as ultrasounds, which typically starts at a lower bound of approximately 18 KHz. As the ultrasound frequency increases, the wavelength decreases allowing for a higher degree of measurement accuracy and resolution that would be necessary for applications such as medical ultrasonography, which utilizes ultrasound frequencies between 2 and 20 MHz. When an ultrasound signal travels from one material medium into another different medium, a percentage of the signal-energy passes through to the other medium, while the rest of the energy is reflected back. Given the speed of ultrasound signals in various material densities, and by measuring the properties of the reflected signal, such as time-difference-of-arrival (TDOA) and signal magnitude, we can calculate some useful information about the examined material, such as volume, thickness, number of various mediums, temperature, and more. NDT has been extensively utilized in a wide range of applications including healthcare, agriculture, defense, manufacturing, fisheries, quality control, cleaning, and many more. By combining WSN technology [1] and the wide use of NDT-based technology, new application domains can potentially unfold.

* Corresponding author. Tel.: "+1-613-533-6000 ext. 78232" ; fax: +1-613-533-6513 .
E-mail address: elkouche@cs.queensu.ca (A. El Kouche) hossam@cs.queensu.ca (H. Hassanein)

doi:10.1016/j.procs.2012.06.021

2. Introduction to Piezoelectric Transducers

Ultrasound waves are generated by applying a short voltage pulse, approximately less than 5ηs, across a Piezoelectric (PZT) material. The voltage pulse generates a very wide frequency band relative to the PZT material, which causes the PZT material to mechanically vibrate at its designed resonant frequency. The generated ultrasound energy is then transferred from the PZT material into the surrounding medium. For example, if the PZT material is formed into a thin disc shape, then most of the generated ultrasound energy will travel from the upper and lower surfaces of the disc. The PZT disc is polarized by the manufacturer during the production process, such that the positive and negative poles are electrostatically coated with a thin layer of silver deposit to allow for easy electrical connections. The negative pole can be grounded to the transducer's metallic packaging to facilitate simple packaging, as seen in Figure 1 (a). When a voltage pulse (V_{pulse}) is applied across the poles of the PZT material, the mechanical vibration is stretched over time as it slowly decreases in magnitude; a behavior similar to the ringing-effect of a metal bell when stroked. For most applications, the ringing-effect is an undesirable outcome since the reflected ultrasound can arrive before the ringing is adequately damped if the material is thin. Therefore, techniques such as dampening-material, or backing-material, is applied to the back side of the PZT disc to greatly reduce the number of resonant cycles produced. The backing-material, however, also dampens the signal amplitude of the generated ultrasound wave, which is an undesired outcome. With adequate dampening, or smaller numbers of cycles produced, we can achieve higher measurement resolution in order to test thinner material, or distinguish finer details of the material under test.

The thickness of the piezoelectric transducer (T_t) and the velocity of sound in the given piezoelectric transducer (υ_t) determine the transducer's resonant frequency (f), as described by equation (1) [2]. The wave length (λ) of the ultrasound signal is inversely proportional to the resonant frequency and dependant on the velocity of sound in the material under test (υ_m), as shown in equation (2) [2]. In order to protect the exposed PZT surface from prolonged physical damage, a wear-plate is interfaced to the front face of the PZT. In addition, the wear-plate has an important role in acting as a matching-layer between the PZT material and the material under test. The recommended thickness of the wear-plate is ¼ λ calculated from equation 2, and has an optimum acoustic impedance Z_w, expressed in units of MRayls $=10^6 Kg/(s.m^2)$, which lies between the acoustic impedance of the transducer Z_t and the acoustic impedance of the material under test Z_m, as described in equation (3)[2].

$$f = \frac{\upsilon_t}{2T_t} \quad (1) \qquad \lambda = \frac{\upsilon_m}{f} \quad (2) \qquad Z_w = \sqrt{Z_t Z_m} \quad (3)$$

In order to measure the thickness of a given material using ultrasound, such as a metal bar, a pulse-echo technique is used. This technique is established by starting a timer at the same time the ultrasound pulse is generated, and consequently stopping the timer when the echoed pulse is detected. The measured time is referred to as the time difference of arrival (TDOA). By multiplying TDOA by the ultrasound velocity in the given known material, we calculate the total travelled distance of the ultrasound wave, which is twice the thickness of the material, as seen in Figure 1 (a). The ultrasound pulse will echo back and forth in the measured material until the amplitude is adequately attenuated as it travels through the material, as depicted in Figure 1 (b). The TDOA between the echoes can be measured and averaged to obtain an averaged reading of the material thickness.

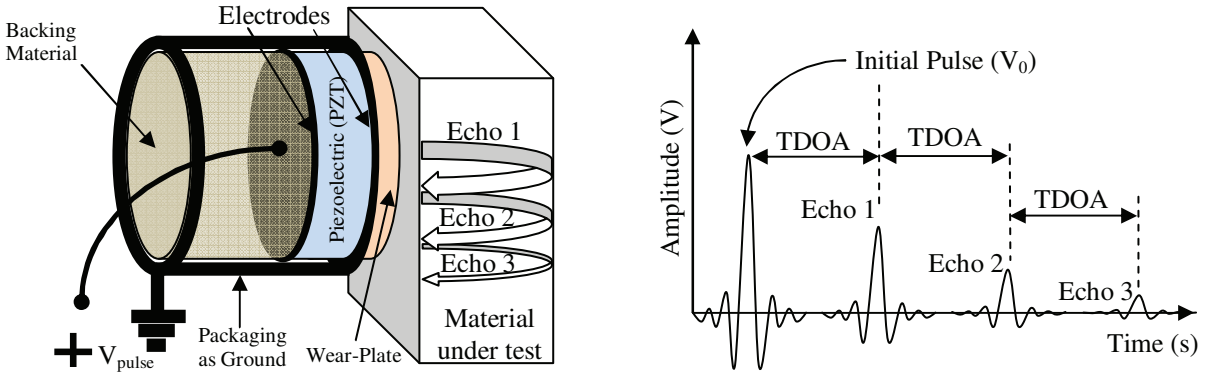

(a) Typical ultrasound transducer construction (b) Pulse-echo technique in measuring thickness

Fig. 1 (a) Typical piezoelectric transducer (b) Generated ultrasound signal echoes from pulse-echo technique

3. Ultrasound Thickness Measurements Using WSNs

Commercially available ultrasound-based NDT equipments are typically too large, power-intensive, and expensive for WSNs. Even handheld NDT equipment, considered to be low cost and portable, typically average around $1,000 per unit (e.g. TG110), and can vary up to several hundred thousands of dollars for a graphical-based flaw detection device. Graphically displaying measured data on a colored display in real-time is a power intensive process that requires very high sampling analog to digital converters (ADCs) and sophisticated graphical display technology. This is a process not required for a WSN since raw data is wirelessly reported back to a server where it is displayed only when needed. Therefore, the only required part of an NDT system is the ultrasound front-end, which is the generation of the ultrasound signal and its timely reception. This significantly reduces power consumption, size, and cost of a WSN-based NDT system. Furthermore, high speed ADCs would not be required for thickness-based NDT, which significantly reduces power burdens on the system. Applications of a WSN-based NDT solution would be most suitable for low cost monitoring of material thickness in a mobile, or static, remote environments, where constant monitoring over an extended period of time, while in operation, is essential. For example, a WSN-based NDT can be utilized to monitor the thickness of hydrotransport metal pipes, monitoring of equipment integrity in harsh environments, monitoring the thickness of excavation shovel teeth while in operation, monitoring for cracks in bridges, etc.

Our unique system architecture for a WSN-based NDT solution builds upon our wireless sensor network platform, called Sprouts [3], which is described in section 3.2. Sprouts is a modular WSN platform that allows up to four custom modules to be externally attached and automatically detected. Modules communicate with Sprouts using plug-and-play (PnP) protocol over a standard serial peripheral interface (SPI) bus. Our unique NDT solution is designed in the form of an external module, which is described in section 3.1.

3.1. NDT-Module System Architecture

Our NDT-module is low cost, low power, reconfigurable, and reliable solution to monitor the thickness of materials, structures, or equipments while in operation. The NDT-module works in conjunction with our Sprouts platform as an attachable external module to one of four module-ports. The NDT-module communicates with Sprouts via custom designed PnP protocol over a standard SPI-bus. The system architecture of the NDT-module is depicted in Figure 2.

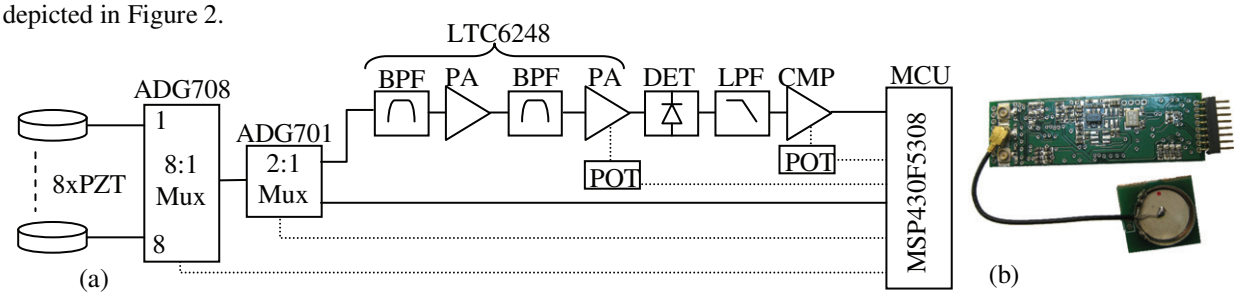

Fig. 2 (a) General system architecture of the NDT-module. Solid lines indicate analog signal paths and dotted lines indicate digital control signals (b) Picture of the NDT-module with one attached PZT transducer

Starting from the far left of Figure 2(a), the NDT-module system architecture is composed of multiple piezoelectric transducers (PZTs), up to 8 channels, which can be selected using a bidirectional 8:1 multiplexer (Mux), ADG708. The PZT transducers have a resonant frequency of 5MHz (±5%), SMD10T04F5000S111, and 10x0.4mm disc size. Multiple channels available per NDT-module introduce many system benefits including:

1) Increased number of monitored locations per NDT-module.
2) Increased reliability with increased redundancy for applications requiring fewer channels.
3) Lowers system costs since one NDT-module can monitor multiple locations.
4) Reduces the required space needed in a given application otherwise occupied by multiple NDT-modules.
5) Lowers power consumption otherwise required by multiple NDT-modules.
6) Increases design flexibility and application spectrum since not all 8 channels need to be utilized.

The second multiplexer is a 2:1 bidirectional Mux, ADG701, which is responsible for switching between two different signal paths leading to, or from, the PZTs. The first path comes from the microcontroller unit (MCU) and connects to one of the selected channels. The MCU generates the short voltage pulse which causes the PZT to resonate at its designed frequency. A simple transition from a digital-low voltage to a digital-high voltage from one of the MCU's digital ports satisfies this requirement. When the pulse is applied to the PZT material, a short pause equal to the duration of the PZT ringing time is applied before switching the 2:1 Mux to the second path. The second path of the 2:1 Mux connects one of the PZT channels to the receiver path of the NDT-module starting with the band pass filter (BPF). The BPF is essential when working in very noisy environments or while monitoring a machine under operation, such as a motor. Both BPFs are Sallen-Key (SK) active-type filters, such that each BPF is designed with a -6dB bandwidth of approximately 1.52MHz centred at approximately 5.10MHz, as seen in Figure 5(a). Any signal outside the bandwidth of the BPF is greatly attenuated before reaching the low noise amplifier (LNA). The LNA has a low input voltage noise density of 4.2ηV/√Hz and a fixed gain of 20dB. The LNA is responsible for amplifying the echo ultrasound signal without introducing too much noise. Noise analysis of the LNA is beyond the scope of this paper. The power amplifier (PA) has a digitally controlled gain from 15dB to 30dB using a 2.1KΩ digital potentiometer (POT) MCP4012 to control gain. The two active SK-BPFs, LNA, and the PA are designed using a single chip, the LTC6248, which contains four operational amplifiers, one for each component. This single chip approach minimizes system cost and circuit space. Each operational amplifier consumes approximately 1mA in active mode, such that the total power consumption of the NDT-module is approximately 6mA at 3.0V, and is only active for less than 0.2ms per channel measurement. The schottky diode envelope detector (DET) rectifies the ultrasound signal, which is then smoothed by a passive low pass filter (LPF) with a -3dB corner frequency of 3MHz. A comparator (CMP), TS3021, is used to detect the presence of the ultrasound signal, such that it transforms the analog echo signal into a digital pulse representing the presence and approximate width of the echoed ultrasound signal. The CMP reference voltage is also controlled by a 2.1KΩ digital POT (MCP4012). The digital output of the CMP is connected to the internal capture-compare (CC) module of the MCU. The CC module is configured to measure the time difference of arrival (TDOA) between two consecutive pulses from the CMP, that is, two consecutive ultrasound echoes. The TDOA (i.e. Δt) is a direct representation of the measured thickness T per given medium with a sound velocity υ, as described in equation 4. Note that Δt is divided by 2 since the ultrasound signal travels twice the thickness of the material.

$$T = \frac{\Delta t}{2}\upsilon \qquad (4)$$

When two consecutive signals are captured by the CC, an interrupt is generated and a 16-bit register records the Δt value. Therefore, the maximum Δt value that can be captured is equal to the period of the clock-frequency driving the CC timer multiplied by 2^{16}. For example, using a 32MHz clock for the MCU, the maximum Δt value is approximately 2048μs, which is enough time to measure a steel-bar (υ=5769m/s) thickness of approximately 590cm. The MCU is a low cost and ultra low power MSP430F5308, which controls the two digital POTs, the two multiplexers, provides power to the ultrasound front end, and generates the voltage pulse for the PZTs. In addition, the MCU reports the thickness per channel when requested by the Sprouts platform using our PnP protocol over an SPI-bus. Using an SPI-bus eliminates the need for accurate timing and allows modules without a crystal-clock to communicate reliably.

3.2. Sprouts System Architecture

Sprouts is a WSN platform with a versatile system architecture designed with modular PnP features throughout its hardware and software layers. The platform was designed to address important key features essential for applications enabling the Internet of Things (IoT). Sprouts emphasizes small physical dimensions, rugged packaging, ultra low power, modularity, PnP operation, energy harvesting, and remote triggering, which are all important features for industrial use. The hardware architecture is designed with modular and interchangeable layers as seen in Figure 3. Sprouts hardware architecture layers and features are described as follows:

1) Magnetic Layer: Sprouts utilizes a strong disc magnet (neodymium 20x2mm) to easily attach the platform on metallic surfaces. This allows for easy deployment in industrial environments.
2) Sensor layer: The sensor layer provides access to our standard PnP protocol. There are four communication ports to attach external modules. This allows for easy PnP customization of the platform per applications.

3) CPU and RF Layer: The CPU and RF layer hosts the local ARM Cortex M3 microcontroller unit (MCU) EFM32G230F128, as well as the Bluetooth Low Energy (BLE) transceiver (Tx/Rx) nRF8001. This is considered the core layer, which cannot be replaced.
4) Harvesting Layer: The energy harvesting layer is responsible for scavenging ambient energy from the environment and converting it into usable electrical energy. Multiple energy harvesting sources can be utilized such as wireless power transfer (WPT), which is also used for remote wakeups, and vibration energy harvesting (VEH) [5].
5) Custom Layer: an application dependent custom layer can be added as necessary. This will allow customization to be packaged inside the rugged housing. Most customizations can also be accomplished using attachable modules
6) Backup Battery: In some situations, energy harvesting might be scarce, unavailable, or excessively abundant. Having a backup battery allows the platform to run exclusively from the battery when energy harvesting is low, or recharge a small coin battery, such as ML-2020, when excessive energy is available.
7) Patch Antenna: the antenna is an important part of the platform. Sprouts utilizes a flat patch antenna, seen in Figure 1 D, which also serves as a cover for the metallic package. The unique advantage of patch antennas is the bottom ground layer which allows the platform to be mounted on metal without effecting reception. In addition, patch antennas are flat and do not exhibit any mechanical moving parts making them better suited for harsh industrial environments.
8) Packaging: Sprouts uses a cylindrical aluminum, copper, or steel packaging 23mm in diameter and only 10mm in height, allowing the package to be light and robust.

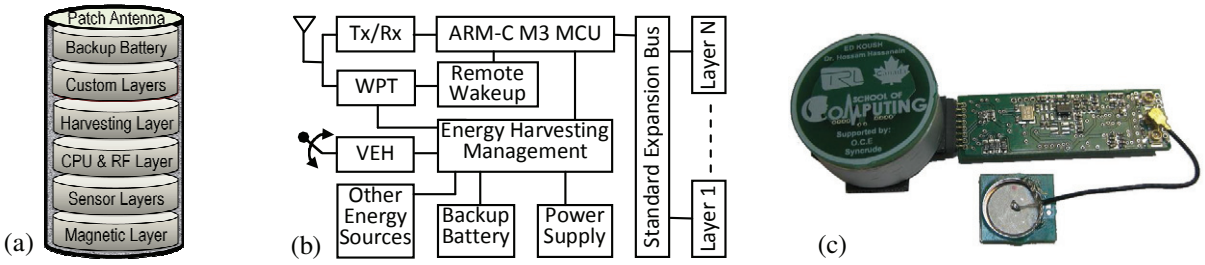

Fig. 3 (a) Sprouts' stacked layer (b) Sprouts' hardware architecture (c) Pictures of Sprouts platform with NDT-module attached

Sprouts builds upon our Dynamically Reconfigurable Energy Aware Middleware Software (DREAMS) architecture as described in [4]. The DREAMS architecture is based on modular software components that can be remotely uploaded and configured based on the amount of energy available and the rate in which energy is harvested. The DREAMS architecture simplifies middleware architecture implementation complexity, decreases faults associated with low energy sources, and increases design flexibility associated with remote upgrades.

4. WSN-based NDT Application

Our WSN-based NDT solution was tested in the harsh operating environment of the Oil Sands, northern Alberta, Canada, to monitor the thickness of the steel mesh in the deployed vibration screens, as described in [5]. The steel mesh is coated with a thin tungsten layer to prolong the operational lifetime of the mesh screen. The main responsibility of the vibration screens is to filter out large ores from the tar-sand. After an extended period of time, approximately 2000 hours, the tungsten layer is completely etched away by the constant flow of sand, thus, exposing the steel layer. The steel layer is much weaker than the tungsten layer, and can be completely etched away within few days of exposure. Critically low levels of steel thickness can break off forming larger screen holes, where large ores can sift through causing damage and congestion to the hydrotransport pipes. At this point, the production process must be halted for an extended period of time for repairs, which leads to significant production loss. Previous to our solution, maintenance checks where manually performed by a an operator whom would visually inspect the thickness of the tungsten and steel layer, and draw a conclusion whether to change the sheet or not based on experience. This technique incurs mental pressure on the inspector to make the right decision, which often leads

to premature screen replacements. In addition, manual checkups require the physical presence of an inspector, the production process must be halted, and the screens must be washed, which is a laborious process that can be omitted using our WSN-based NDT solution.

To measure the thickness of the vibration screen ligaments, Sprouts nodes and NDT-modules are placed on the steel layer underneath the mesh screen at each intersection, where they are shielded from direct contact with the sand flow. When a thickness measurement is needed, Sprouts nodes request thickness readings from each channel of the NDT-module or from all channels as specified by the server configuration. When a thickness reading is requested from a particular channel, the NDT-module applies a fast voltage pulse to the PZT transducer by toggling a digital logic port from low to high. The fast transition from logic-low to logic-high, less than 5.0ηs rise time, creates a wideband frequency response, which causes the PZT transducer (SMD10T04F5000S111) to resonate at approximately 5MHz (±5%) with initial pulse magnitude voltage V_0, as seen in Figure 5 (a). The initial pulse, which occurs at time t_0, travels through the steel layer until it reaches the end of the material boundary or a material of different density, such as the tungsten layer, at time t_a. The mismatch in material density causes a percentage of the ultrasound energy, R_1, to be reflected back to the transducer proportional to the acoustic impedance mismatch between steel (Z_1= 45.63MRayls) and tungsten (Z_2= 99.72MRayls), as shown in equation (5)[2]. Therefore, at the boundary between the two metals, or time location t_a, the percentage of reflected energy is R_1=0.1385, or 13.85%. Acoustic impedance is a function of material density ρ and velocity of sound, υ, in the given material, as shown in equation (6). Note that ρ and υ for a given material, such as steel or tungsten, can vary depending on manufacturing.

$$R = \left(\frac{Z_1 - Z_2}{Z_1 + Z_2} \right)^2 \qquad (5) \qquad Z = \rho \upsilon \qquad (6)$$

The reflected percentage of ultrasound energy, R_1, travels from time location t_a to arrive back at the PZT transducer at time location t_1 where it can be measured as amplitude V_1 from the electrodes. The TDOA between the initial pulse and first received echo is $\Delta t_1 = t_1 - t_0$, which is used to measure the steel thickness T_1, as described in equation (4). The remaining percentage of energy, R_2=86.15%, travels through the tungsten layer until it reaches the second boundary, air, at time location t_b, which has very low acoustic impedance of 0.0004 MRayls. Due to the very large difference in acoustic impedance between air and tungsten, the signal energy is completely reflected back into the tungsten material travelling towards the steel layer. When the signal reaches the tungsten-steel boundary at time location t_c, another percentage energy R_1 is reflected back, however, this time it is reflected back into the tungsten layer. The remaining percentage of energy R_2, makes its way through the steel layer to arrive back at the transducer at time t_2 with voltage magnitude V_2. The TDOA $\Delta t_2 = t_2 - t_1$ is used in equation (4) to measure the thickness of the tungsten layer T_2. Note that the ultrasound signal at time location t_2 will be reflected again into the steel, such that the whole cycle is repeated until all signals are attenuated according to equation (7), where V is the exponential decrease in voltage amplitude of the sound signal at distance d, and V_0 is the initial voltage amplitude produced by the PZT at t_0. The attenuation coefficient α, expressed in dB/cm, is dependent on the PZT resonant frequency and varies with manufacturer processing technology. Therefore, α is experimentally calculated by measuring the initial voltage sample V_i and a final voltage sample V_f separated by distance d according to equation (8).

$$V = V_0 e^{\alpha . d} \qquad (7) \qquad \alpha = \frac{20}{d} Log\left(\frac{V_i}{V_f}\right) \qquad (8)$$

Since voltage signals can only be measured from the PZT transducer's electrodes, we calculate the voltage magnitude V_a at t_a, in equation (9), right before entering the tungsten medium. Similarly, we derive an expression for V_1 at t_1 as seen in equation (10).

$$V_a = V_0 e^{\alpha_1 . T_1} \qquad (9) \qquad V_1 = R \times V_a e^{\alpha_1 . T_1} \qquad (10)$$

Dividing equation (9) by equation (10), we obtain equation (11), an expression for V_a that is independent of T_1 and α_1.

$$V_a = \sqrt{\frac{V_0 V_1}{R}} \qquad (11)$$

Using equation (8), such that V_i is equivalent to V_0, V_f is equivalent to V_a, and d is T_1, we derive the steel's attenuation coefficient α_1 using equation (11) as a function of measurable voltages V_0 and V_1.

$$\alpha_1 = \frac{20}{T_1} Log\left(\sqrt{\frac{RV_0}{V_1}}\right) \quad (12)$$

In order to find the attenuation coefficient of tungsten, α_2, we represent V_c as the signal amplitude at point t_c right before entering the steel medium, such that:

$$V_c = (1-R)\times V_a e^{2\alpha_2 . T_2} \quad (13) \qquad V_2 = (1-R)\times V_c e^{\alpha_1 . T_1} \quad (14)$$

As described earlier, the signal is completely reflected at time location t_b. Thus, the signal travels twice the thickness of tungsten T_2 from point V_a to point V_c without an R loss at time location t_b. Using equation (8), such that V_i is equivalent to $(1\text{-}R)V_a$, V_f is equivalent to V_c, and d is twice the thickness of tungsten T_2, we derive an expression for α_2 from equations (9-14) as a function of measurable voltages V_1 and V_2.

$$\alpha_2 = \frac{10}{T_2} Log\left(\frac{(1-R)^2}{R}\times\frac{V_1}{V_2}\right) \quad (15)$$

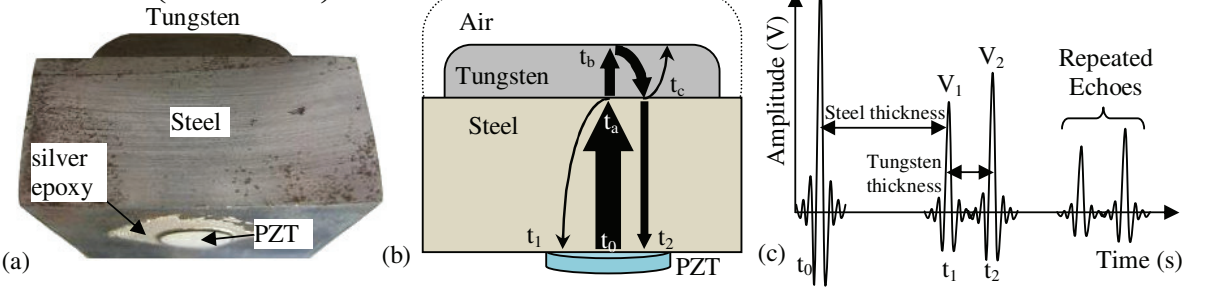

Fig. 4 (a) Cross-sectional lab-sample of steel and tungsten layers (b) Ultrasound reflections and time locations as it travels through the steel and tungsten layers (not drawn to scale) (c) Representation of the ultrasound echoes at the PZT electrodes

Using an oscilloscope for calibration and verification purposes, we measured the initial voltage V_0=448mV from Figure 5(a), at time location t_0. From Figure 5(b), we measured reflected voltages V_1=30.4mV at time location t_1 and V_2=70.4mV at time location t_2. We measured Δt_1=6.76µs from Figure 5(a-b), and from Figure 5(b) we measured Δt_2= 1.440µs. Knowing the actual thickness of steel=19.50mm and tungsten=3.85mm, we calibrated for υ_1=5769m/s and υ_2=5347m/s using equation (4) and measured Δt_1 and Δt_2 from the oscilloscope. Our measurement results of υ_1=5769m/s and υ_2=5347m/s for steel and tungsten closely match the values found in [2] (i.e. υ_1=5890 m/s, υ_2=5180 m/s), such that the slight difference is due to the manufacturing process of the two metals. Using equations (12) and (15) we calculated signal losses in the two mediums α_1=1.59dB/cm, and α_2=9.46dB/cm. Thus, the total signal loss through the two mediums is 13.4dB for one echo reflection. Another 16.5dB is required to bring the 448mV to a rail-to-rail voltage swing of 3.0V; thus, a minimum gain of approximately 30dB was needed. Since other factors in the NDT-module design will contribute to the echo signal loss, such as the Muxes, two BPFs, DET, and LPF, the digitally controlled PA compensates for approximately 15dB of dynamic range.

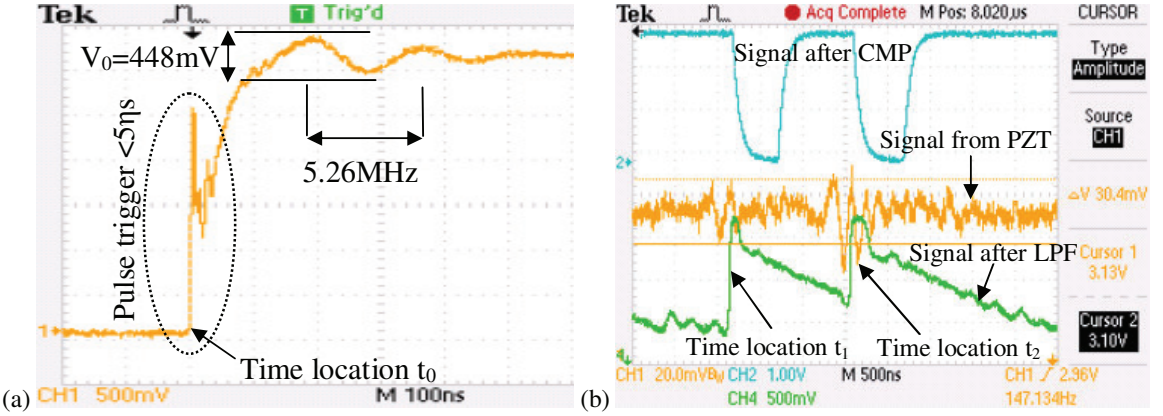

Fig. 5 (a) Fast pulse trigger excites the PZT at its resonant frequency (b) Ultrasound echo signals at the PZT, after the LPF, and after CMP

A summary of results for our NDT-module solution are shown in Table 1, which draws a comparison between our ultrasound-based measured results using low power MSP430 solution, and the actual thickness of the steel and tungsten layer. The error percentage is due to the finite resolution of the MCU's CC module, which operates at a maximum clock speed of 32MHz, or 31.25ηs per clock tick. Increasing the resolution of the CC would require a different MCU with higher maximum clock speeds, which comes at the cost of increased power consumption.

Table 1 Summary of results for our WSN-based NDT-module

Measurement	***Steel***	***Tungsten***
Actual Thickness	19.50 mm	3.85 mm
NDT-module measured	19.56 mm	3.93 mm
Max Thickness Error %	0.31%	2.0%
Longitudinal Velocity	5769 m/s	5347 m/s
Attenuation Coefficient	1.59 dB/cm	9.46 dB/cm

The summary of results in Table 1 show a promising approach for using low cost and ultra low power wireless sensor nodes to perform NDT-based measurements, such that percentage errors are relatively very low. Increased accuracy can be attained by increasing the clock frequency of the MCU at the cost of increased power consumption. Applications that can tolerate percentage errors presented in Table 1 can greatly benefit from WSN-based NDT by having the low cost wireless capability of monitoring equipment or material while in operation without the use of wired and expensive NDT equipment.

5. Conclusion

We have presented the system architecture to allow for low power and low cost ultrasonic NDT using WSNs. Our NDT solution is developed as a modular architecture with PnP capabilities provided by our previous work on Sprouts. The NDT-module was used to measures the thickness of the steel and tungsten layers in a compound metal structure. We have shown analytical and experimental analysis to verify our working solution. Our application results show that for thickness based measurements, accuracy of measurements using low power sensor nodes, such as MSP430 MCUs, can be as high as 99.69% for a steel bar of 19.5mm thickness. This introduces a new promising application domain in using ultra low power MCUs in WSN nodes for NDT-based measurements applicable in industrial, scientific, or commercial domains, where equipment, material, or structures can be monitored in real-time using wirelessly, low cost, and low power wireless sensor nodes.

Acknowledgements

This research work was conducted at the Telecommunication Research Lab (TRL) at Queen's University. This project was funded by the Natural Sciences and Engineering Research Council of Canada (NSERC).

References

[1] I. Akyildiz et al., "A Survey on Sensor Networks," IEEE Commun. Mag., vol. 40, no. 8, pp. 102–14, 2002.

[2] P.O. Moore, G.L. Workman, D. Kishoni, "Nondestructive Testing Handbook: Ultrasonic Testing," 3rd ed., vol.7, ASNT, 2007.

[3] A. El Kouche, "Towards a Wireless Sensor Network Platform for the Internet of Things," IEEE ICC 2012, Ottawa, Canada, accepted.

[4] A. El Kouche, L Al-Awami, H. Hassanein,"Dynamically Reconfigurable Energy Aware Modular Software (DREAMS) Architecture for WSNs in Industrial Environments," Ambient Sys.Net.and Tech. (ANT), Aug 2011.

[5] A. El Kouche, L. Al-Awami, H. Hassanein, K. Obaia, "WSN application in the harsh industrial environment of the oil sands," IWCMC, July 2011.